REFERENCES AND NOTES

1. J. D. McKinney and N. Heintz, *Trends Biochem. Sci.* **16**, 430 (1991).
2. S. Ruppert, E. H. Wang, R. Tjian, *Nature* **362**, 175 (1993).
3. K. Hisatake *et al.*, *ibid.*, p. 179.
4. N. Tanese, B. F. Pugh, R. Tjian, *Genes Dev.* **5**, 2212 (1991).
5. B. F. Pugh and R. Tjian, *ibid.*, p. 1935.
6. T. Sekiguchi, T. Miyata, T. Nishimoto, *EMBO J.* **7**, 1683 (1988).
7. T. Sekiguchi, Y. Nohiro, Y. Nakamura, N. Hisamoto, T. Nishimoto, *Mol. Cell. Biol.* 11, 3317 (1991).
8. A. Talavera and C. Basilico, *J. Cell. Physiol.* **92**, 425 (1977).
9. B. D. Dynlacht, T. Hoey, R. Tjian, *Cell* **66**, 563 (1991).
10. Q. Zhou, P. M. Lieberman, T. G. Boyer, A. J. Berk, *Genes Dev.* **6**, 1964 (1992).
11. H. T. Liu *et al.*, *J. Biol. Chem.* **260**, 3269 (1985).
12. For the preparation of nuclear extracts, ts13 cells were synchronized by serum starvation and subsequently induced with 10% fetal bovine serum at the permissive (33.5°C) or nonpermissive (39.5°C) temperature as described (*8*). After 20 to 24 hours of growth, nuclear extracts were prepared according to the method of Dignam *et al.* [J. D. Dignam, R. M. Lebovitz, R. G. Roeder, *Nucleic Acids Res.* 11, 1475 (1983)]. Nuclear extracts were also prepared from BHK-21 cells grown at 37°C.
13. The pCMVGR vector contains rat GR under the control of the cytomegalovirus promoter-enhancer [C. M. Gorman, D. Gies, G. McCray, M. Huang, *Virology* 171, 377 (1989)]. The pCMVhTAF$_{II}$250 vector was constructed by replacement of the coding region of rat GR in pCMVGR with that of hTAF$_{II}$250. The ts13 cells plated on 6-cm dishes were transfected in duplicate with either 12 μg of pCMVGR or 20 μg of pCMVhTAF$_{II}$250 by calcium phosphate precipitation. After 16 hours at 33.5°C, half of the cells were shifted to 39.5°C. After 4 days at 33.5°C or 7 days at 39.5°C, photomicrographs were taken at ×125 magnification.
14. E. H. Wang and R. Tjian, unpublished data.
15. T. Sekiguchi, M. C. Yoshida, M. Sekiguchi, T. Nishimoto, *Exp. Cell Res.* **169**, 395 (1987).
16. T. Sekiguchi, personal communication.
17. R. O. J. Weinzierl, B. D. Dynlacht, R. Tjian, *Nature* **362**, 511 (1993).
18. T. Kokubo, D.-W. Gong, R. G. Roeder, M. Horidoshi, Y. Naktani, *Proc. Natl. Acad. Sci. U.S.A.* **90**, 5896 (1993).
19. T. Hoey *et al.*, *Cell* **72**, 247 (1993).
20. J. A. Goodrich, T. Hoey, C. J. Thut, A. Admon, R. Tjian, *ibid.* **75**, 519 (1993).
21. F. Girard, U. Strausfeld, A. Fernandez, N. J. C. Lamb, *ibid.* **67**, 1169 (1991).
22. M. Ustav and A. Stenlund, *EMBO J.* **10**, 449 (1991).
23. L. Yang, R. Li, I. J. Mohr, R. Clark, M. R. Botchan, *Nature* **353**, 628 (1991).
24. K. A. Jones, J. T. Kadonaga, P. J. Rosenfeld, T. J. Kelly, R. Tjian, *Cell* **48**, 79 (1987).
25. S. Shirodkar *et al.*, *ibid.* **68**, 157 (1992).
26. T. Sekiguchi, personal communication.
27. Transcription assays were done essentially as described [B. F. Pugh and R. Tjian, *Cell* **61**, 1187 (1990)]. Reaction mixtures (25 μl) containing 10-ng template DNA, 50 to 100 μg of nuclear extract, 200 ng of nonspecific DNA (pBS+), and either 50 ng of Gal4VP16 or 100 ng of Sp1 where indicated, were preincubated for 30 min at the indicated temperature in the absence of ribonucleoside triphosphates (NTPs). After the addition of NTPs to a final concentration of 0.5 mM, the reaction was allowed to proceed for an additional 10 to 15 min. The products were detected by primer extension, followed by denaturing polyacrylamide gel electrophoresis, and visualized by autoradiography. The DNA template containing five Gal4-binding sites upstream of the adenovirus E4 promoter (G_5E4T) has been described [Y.-S. Lin, M. F. Carey, M. Ptashne, M. R. Green, *Cell* **54**, 659 (1988)]. GCE4T was constructed by insertion of the six GC boxes from SV40 upstream of the adenovirus E4 promoter in the E4T template.
28. S. M. Lobo, M. Tanaka, M. L. Sullivan, N. Hernandez, *Cell* 71, 1029 (1992).
29. M. Z. Gilman, R. N. Wilson, R. A. Weinberg, *Mol. Cell. Biol.* **6**, 4305 (1986).
30. P. Herbomel, B. Bourachot, M. Yaniv, *Cell* **39**, 653 (1984).
31. J. R. Neuman, C. A. Morency, K. O. Russian, *BioTechniques* **5**, 444 (1987).
32. R. A. Hipskind and A. Nordheim, *J. Biol. Chem.* **266**, 19583 (1991).
33. We are indebted to C. Basilico for providing the ts13 cell line and B. Johnson for technical assistance in tissue culture. We thank J. Goodrich for providing purified Gal4VP16, J.-L. Chen for purified Sp1, N. Tanese for 1.0 M KCl fraction of LTRα3 cells, G. Gill for the GCE4T and G_5E4T DNA templates, Genentech for the use of the pCMVGR expression vector, S. Ruppert for constructing pCMVhTAF$_{II}$250, T. Nikaido for the human cyclin A promoter, and M. Gilman for the mouse c-fos promoter. The SL33 monoclonal antibody and the antibody to hTAF$_{II}$250 peptide were provided by N. Hernandez and T. Sekiguchi, respectively. We also thank the lab of D. Rio for help with and use of their photomicrographic apparatus. We especially thank J. Goodrich, S. Ruppert, G. Gill, J.-L. Chen, and members of the Tjian lab for valuable discussions and for critically reading the manuscript. E.H.W. was supported by a postdoctoral fellowship from the American Cancer Society (grant PF-3686). Funded in part by a grant from the NIH to R.T.

31 August 1993; accepted 23 December 1993

Mapping the Lectin-Like Activity of Tumor Necrosis Factor

Rudolf Lucas,* Stefan Magez, Robert De Leys, Lucie Fransen, Jean-Pierre Scheerlinck, Murielle Rampelberg, Erwin Sablon, Patrick De Baetselier

Tumor necrosis factor (TNF), but not lymphotoxin (LT), is directly trypanolytic for salivarian trypanosomes. This activity was not blocked by soluble 55-kilodalton and 75-kilodalton TNF receptors, but was potently inhibited by *N,N'*-diacetylchitobiose, an oligosaccharide that binds TNF. Comparative sequence analysis of TNF and LT localized the trypanocidal region, and synthetic peptides were trypanolytic. TNF molecules in which the trypanocidal region was mutated or deleted retained tumoricidal activity. Thus, trypanosome-TNF interactions occur via a TNF domain, probably with lectin-like affinity, which is functionally and spatially distinct from the mammalian TNF receptor binding sites.

The pleiotropic cytokine TNF has numerous effects on mammalian cells, initiated by binding to high-affinity receptors (*1*). In addition to binding to mammalian 55-kD and 75-kD receptors, TNF has a lectin-like specificity (*2*), the physiological relevance of which remains to be determined. TNF interacts directly with certain parasites (*3, 4*) as well as bacteria (*5*): In the case of the pathogenic bacteria *Shigella flexneri*, the interaction does not involve molecules comparable to the classical mammalian TNF receptors, implying the existence of an alternative recognition domain of TNF for bacterial components. The lectin-like activity of TNF represents a possible candidate for such an alternative recognition, since it is completely dissociable from the tumoricidal activity (*2*).

This study defines the region of TNF that interacts with salivarian trypanosomes. TNF inhibits the development of *Trypanosoma brucei brucei* in vivo (*6*) and in vitro: Both mouse and human TNF (m/hTNF), but not human lymphotoxin (hLT), are trypanolytic for purified bloodstream forms of *T. brucei brucei* (Fig. 1A). Preincubation of mTNF with soluble extract of *T. brucei brucei* potently inhibited the trypanolytic activity (Fig. 1A) without affecting the tumoricidal activity on L929 cells (Fig. 1B). These results indicate that mTNF interacts with *T. brucei brucei* and that this interaction does not interfere with the binding of mTNF to the mouse 55-kD TNF receptor, which mediates the bioactivity of m/hTNF on L929 cells (*7*).

To further substantiate the possibility that the mTNF binding site for the 55-kD TNF receptor is not involved in trypanocidal activity, we performed inhibition experiments with a soluble form of the human 55-kD TNF receptor (shTNF-RI), which binds both hTNF and mTNF (*8*). Preincubation of mTNF with shTNF-RI resulted in a total inhibition of the mTNF tumoricidal activity on L929 cells, but only marginal inhibition of the trypanocidal activity on *T. brucei brucei* (Table 1). Similar results were obtained for a soluble form of the

R. Lucas, S. Magez, J.-P. Scheerlinck, P. De Baetselier, Laboratory of Cellular Immunology, University of Brussels, Campus Rode, Paardenstraat 65, B-1640 Sint-Genesius-Rode, Belgium.
R. De Leys, L. Fransen, E. Sablon, Innogenetics N.V., Industriepark Zwijnaarde 7, Box 4, B-9052 Zwijnaarde, Belgium.
M. Rampelberg, Laboratory of General Biology, University of Brussels, Campus Rode, Paardenstraat 65, B-1640 Sint-Genesius-Rode, Belgium.
*To whom correspondence should be addressed.

human 75-kD TNF receptor (shTNF-RII) on the trypanocidal activity of hTNF. Thus, the two activities of TNF (tumoricidal as compared with trypanocidal) appear to be mediated by different regions of the molecule.

Since m/hTNF, but not hLT, exert trypanolytic activity, we compared the sequence of the molecules in order to identify dissimilar amino acid sequences. The region of mTNF from Ser^{99} to Glu^{115} (Ser^{100} to Glu^{116} in hTNF), which is situated at the upper side of the triangular pyramid shape of TNF, was found to be almost completely absent in both mouse and human LT. The upper side of the hLT molecule is clearly conformationally different from the corresponding region in the hTNF molecule (9).

To assess whether the amino acid region Ser^{99} to Glu^{115} of mTNF is involved in the interaction with trypanosomes, we elicited in rabbits antisera to a synthetic peptide (referred to hereafter as the tip peptide) corresponding to this domain of mTNF. The antisera bound specifically to the mTNF-tip peptide and to native mTNF, indicating that the elicited antibody to tip peptide (anti-tip) reacts with mTNF epitopes. Anti-tip was used to test whether the tip region of mTNF plays a role in the trypanolytic and the tumoricidal activities of mTNF. As shown in Fig. 1A, anti-tip neutralized the trypanolytic activity of mTNF, but exerted only a minor influence on the tumoricidal effect of mTNF (Fig. 1B).

We next investigated whether the TNF-tip peptide alone could exert a trypanolytic activity. As shown in Fig. 2A, both the murine and the human TNF-tip peptide were trypanolytic for bloodstream forms of *T. brucei brucei* (although a 10,000 times higher molar concentration was required to obtain the same degree of lysis as with m/hTNF), whereas they had no tumoricidal effect on L929 cells (*10*). To identify amino acid residues in the tip peptide that were crucial to the trypanolytic activity, we synthesized a tip subpeptide encompassing the amino acid sequence Thr^{104} to Glu^{109} of mTNF (Thr^{105} to Glu^{110} in hTNF), which is identical in mouse and human TNF. As shown in Fig. 2A, the tip subpeptide had full trypanolytic activity. Several amino acid substitution variants of the tip subpeptide were generated in which every amino acid was sequentially replaced by an Ala, and tested in the trypanolysis assay. The replacement of Thr^{104}, Glu^{106}, or Glu^{109} by an Ala residue resulted in a total loss of trypanolytic activity, whereas the replacement of Pro^{105} and Gly^{107} by an Ala residue did not influence the trypanolytic capacity of the tip subpeptide (Fig. 2B).

The functional involvement of the tip region, as well as the amino acid Thr^{104} (Thr^{105} in hTNF), in the trypanolytic activity of mTNF was corroborated with the use of TNF mutants. A deletion mutant of mTNF [del(T^{104}–E^{109})], in which the amino acid positions corresponding to the tip subpeptide were deleted, as well as a Thr^{104} to Ala (T104A) substitution mutant of mTNF, lost most of the trypanolytic activity of mTNF, whereas a Pro^{105} to Ala (P105A) substitution mutant fully retained the trypanolytic activity of wild-type mTNF (Fig. 3). The tumoricidal activity of the del(T^{104}–E^{109}) and the P105A mTNF mutants toward L929 cells was comparable to that of wild-type mTNF (specific activity: wild-type, 1.8×10^8 U/mg; del(T^{104}–E^{109}), 1.49×10^8 U/mg; P105A, 1.8×10^8 U/mg), whereas the T104A mutant had a 50% lower tumoricidal activity (specific activity, 0.91×10^8 U/mg). Thus, these results confirm our observations with the synthetic tip peptides. The region of m/hTNF corresponding to the tip peptide has not been reported to be implicated in the binding to either the 55-kD or the

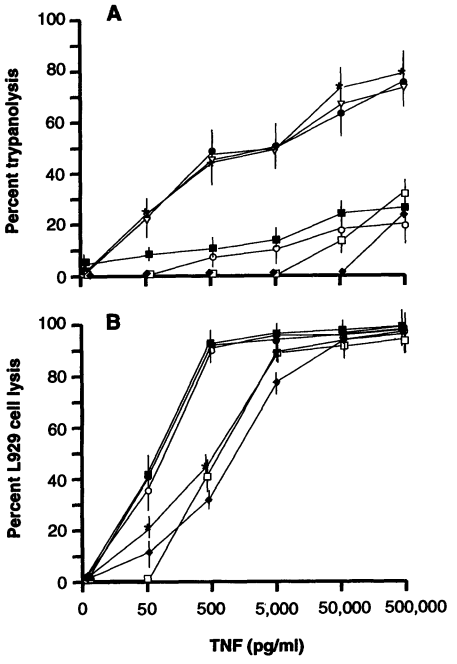

Fig. 1. Comparison of the influence of different agents on the trypanolytic and the tumoricidal activity of TNF. (**A**) Trypanolytic activity of m/hTNF and hLT in vitro on 10^6 purified bloodstream forms of *T. brucei brucei* per milliliter after 5 hours of incubation (*21*): mTNF (●), hTNF (*), hLT (◆), mTNF + lysate (■), mTNF + anti-tip (□), mTNF + irrelevant antibody (▽), and mTNF + *N,N'*-diacetylchitobiose (○). All values represent the means of quadruplicates ± SD. (**B**) Tumoricidal activity of mTNF on L929 cells after 18 hours of incubation in the presence of actinomycin D (1 μg/ml) (*23*). Symbols are as in (A).

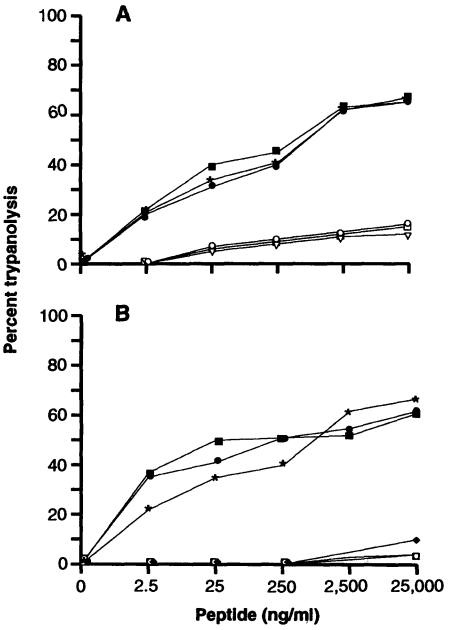

Fig. 2. Trypanolytic activity in vitro of TNF-derived synthetic peptides on purified bloodstream forms of *T. brucei brucei* after 5 hours of incubation (*24*). (**A**) Influence of a 1-hour preincubation with *N,N'*-diacetylchitobiose (1 μg/ml) on the trypanolytic activity of TNF tip-derived peptides: mtip (●), htip (■), and tip subpeptide (*), mtip + *N,N'*-diacetylchitobiose (○), htip + *N,N'*-diacetylchitobiose (□), and tip subpeptide + *N,N'*-diacetylchitobiose (▽). (**B**) Trypanolytic activity of several substitution mutants of the tip subpeptide: tip subpeptide (*), m1 (□), m2 (■), m3 (○), m4 (●), and m5 (◆). All values represent the means of quadruplicates (SD < 8% for all values).

Table 1. Inhibitory capacity (% inhib.) of shTNF-RI on the tumoricidal and trypanocidal activity of mTNF. The mTNF was preincubated with a soluble form of the 55-kD human TNF-receptor (*8*), shTNF-RI (10 μg/ml), before the addition to purified bloodstream forms of *T. brucei brucei* or L929 fibrosarcoma cells. The in vitro trypanolysis assay, as well as the L929 cell lysis assay, are described in Fig. 1.

mTNF (pg/ml)	Trypanocidal activity (% lysis)			Tumoricidal activity (% lysis)		
	−shTNF-RI	+shTNF-RI	% inhib.	−shTNF-RI	+shTNF-RI	% inhib.
100	30 ± 2	25 ± 3	15 ± 5	40 ± 2	0 ± 1	100 ± 5
1,000	45 ± 5	41 ± 4	10 ± 4	92 ± 3	0 ± 1	100 ± 4
10,000	60 ± 4	56 ± 3	7 ± 5	98 ± 4	93 ± 3	5 ± 3

75-kD TNF receptor. In fact, mutational analysis suggests that the receptor binding sites for both TNF receptors are situated in the lower half of its triangular pyramid shape (*11*). Moreover, the tip region is not present in LT, which is capable of binding to both TNF receptors (*12*), suggesting that the involvement of the trypanolytic domain of TNF in the binding to the 55-kD or the 75-kD receptor is unlikely.

As the trypanolytic activity of TNF does not seem to be mediated by surface molecules comparable to the high-affinity TNF receptors on murine cells, and since TNF has been reported to have a lectin-like affinity for *N,N'*-diacetylchitobiose (*2*), we investigated protein-carbohydrate interactions in the trypanolytic activity of mTNF. Preincubation of mTNF or of the trypanolytic peptides with *N,N'*-diacetylchitobiose, but not with cellobiose, results in a potent inhibition of trypanolytic activity (Figs. 1A and 2A) without influencing the tumoricidal activity of mTNF toward L929 cells (Fig. 1B). Moreover, preincubation of the *T. brucei brucei* bloodstream forms with lectins displaying a specificity for *N,N'*-diacetylchitobiose such as *Triticum vulgaris* agglutinin (WGA) (*13*) and *Urtica dioica* agglutinin (UDA) (*14*) inhibited the mTNF trypanolytic activity (Table 2). By contrast, no inhibitory activity was observed with lectins displaying other specificities, such as *Galanthus nivalis* agglutinin (*15*) (GNA) or *Griffonia simplicifolia* A_4 lectin (GSI-A_4) (*16*). These results indicate that the lectin-like activity of mTNF is directly or indirectly involved in its trypanolytic capacity.

The involvement of this lectin-carbohydrate interaction has yet to be studied in the interaction between TNF and other pathogens, such as *Schistosoma mansoni*, *Trypanosoma musculi*, and *Shigella flexneri*. Similarly, the possible physiological function of the lectin-carbohydrate interaction remains to be studied. It is possible, since LT lacks the recognition site, that this region may account for a number of biological activities on endothelial cells (*17*), fibroblasts (*18*), monocytes (*19*), and neutrophils (*20*) that are restricted mainly to TNF.

In conclusion, TNF exerts a direct trypanolytic activity on salivarian trypanosomes by means of a protein-carbohydrate interaction. This activity is mediated by a region of TNF (Thr^{105} to Glu^{110} in hTNF and Thr^{104} to Glu^{109} in mTNF) that has not been implicated in the interaction of this cytokine with either the 55-kD or the 75-kD TNF receptors. This region contains the lectin-like activity of TNF for *N,N'*-diacetylchitobiose. Amino acid residues Thr^{105}, Glu^{107}, and Glu^{110} are of critical functional importance.

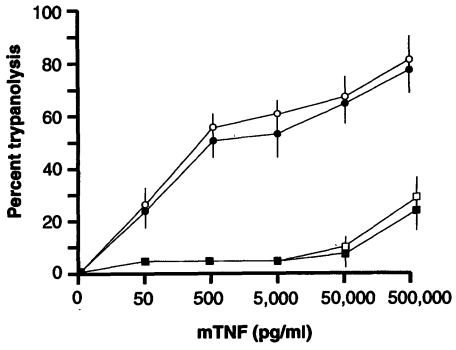

Fig. 3. Trypanolytic activity of T104A and P105A substitution mutants of mTNF and of a (T^{104}–E^{109}) deletion mutant of mTNF [produced as described in (*25*)] in comparison with wild-type mTNF after 5 hours of incubation with bloodstream forms of *T. brucei brucei* (protocol as described in Fig. 1A): mTNF (●), P105A mTNF (○), T104A mTNF (□), and del(TPEGAE) mTNF (■).

Table 2. Inhibitory capacity of different lectins on mTNF-mediated trypanolysis in vitro. The purified trypanosomes were incubated with the indicated lectins (10 μg/ml) 1 hour before the addition of mTNF. WGA (wheat-germ agglutinin), *Triticum vulgaris* agglutinin; UDA, *Urtica dioica* agglutinin; GNA, *Galanthus nivalis* agglutinin; GSI-A_4, *Griffonia simplicifolia* A_4 agglutinin. The in vitro trypanolysis assay was done as described in Fig. 1A.

mTNF (pg/ml)	Percent inhibition of trypanolysis			
	WGA	UDA	GNA	GSI-A_4
100	70 ± 4	80 ± 2	0 ± 1	0 ± 2
1,000	63 ± 5	63 ± 3	5 ± 3	0 ± 2
10,000	13 ± 5	29 ± 5	5 ± 2	2 ± 1
100,000	5 ± 3	3 ± 2	3 ± 2	0 ± 2
1,000,000	7 ± 5	2 ± 1	2 ± 1	0 ± 1

REFERENCES AND NOTES

1. H. Loetscher *et al.*, *Cell* **61**, 351 (1990); C. A. Smith *et al.*, *Science* **248**, 1019 (1990).
2. A. P. Sherblom, J. M. Deckers, A. V. Muchmore, *J. Biol. Chem.* **263**, 5418 (1988); C. Hession *et al.*, *Science* **237**, 1479 (1987).
3. P. Amiri *et al.*, *Nature* **356**, 604 (1992).
4. P. A. Kongshavn and E. Ghadirian, *Parasite Immunol.* **10**, 581 (1988).
5. G. Luo *et al.*, *Infect. Immun.* **61**, 830 (1993).
6. S. Magez, R. Lucas, E. Bajyana-Songa, R. Hamers, P. De Baetselier, *Parasite Immunol.* **15**, 635 (1993).
7. L. A. Tartaglia *et al.*, *Proc. Natl. Acad. Sci. U.S.A.* **88**, 9292 (1991).
8. H. Engelmann, D. Novich, D. Wallach, *J. Biol. Chem.* **265**, 1531 (1990).
9. M. J. Eck, M. Ulthsch, E. Rinderknecht, A. M. de Vos, S. R. Sprang, *ibid.* **267**, 2119 (1992).
10. R. Lucas *et al.*, unpublished results.
11. J. Yamagishi *et al.*, *Protein Eng.* **3**, 713 (1990); X. Van Ostade, J. Tavernier, T. Prangé, W. Fiers, *EMBO J.* **10**, 827 (1991).
12. H.-J. Schoenfeld *et al.*, *J. Biol. Chem.* **266**, 3863 (1991).
13. I. J. Goldstein and C. E. Hayes, *Adv. Carbohydr. Chem. Biochem.* **35**, 127 (1978).
14. N. Shibuya, I. J. Goldstein, J. A. Shafer, W. J. Peumans, W. F. Broekaert, *Arch. Biochem. Biophys.* **249**, 215 (1986).
15. N. Shibuya, I. J. Goldstein, E. J. M. Van Damme, W. J. Peumans, *J. Biol. Chem.* **263**, 728 (1988).
16. C. Wood, E. A. Kabat, L. A. Murphy, I. J. Goldstein, *Arch. Biochem. Biophys.* **198**, 1 (1979).
17. R. M. Locksley *et al.*, *J. Immunol.* **139**, 1891 (1987).
18. H. P. Koeffler *et al.*, *Blood* **70**, 55 (1987).
19. W. Oster, A. Lindemann, S. Horn, R. Mertelsmann, F. Herrman, *ibid.*, p. 1700.
20. N. A. Cicco *et al.*, *ibid.* **75**, 2049 (1990).
21. For the in vitro trypanolysis assay, bloodstream forms of *T. brucei brucei* AnTat 1.1 were isolated from C_3H/He mice injected intraperitoneally on day 0 with 1000 trypanosomes per mouse. The trypanosomes were harvested 1 day before the first peak of parasitemia was reached. Trypanosomes were then purified on a DEAE column as described [M. S. Lanham and D. G. Godfrey, *Exp. Parasitol.* **28**, 521 (1970)] and were incubated in flat-bottomed 96-well plates at a concentration of 10^6 trypanosomes per milliliter in a humid incubator at 37°C and a 5% CO_2 atmosphere in phosphate-buffered saline (PBS) (pH 7.2), supplemented with 1% D-glucose and 1% normal mouse serum. Under these conditions, the observed percentage of trypanolysis in the control wells after 5 hours in incubation medium without TNF was always <10%. We prepared trypanosome soluble extracts by taking the supernatant of trypanosome lysates, obtained by a threefold freeze-thawing procedure, centrifuged at 17,000*g* for 10 min. After 5 hours of incubation in the presence or the absence of hLT and h/mTNF, the latter having been treated or not as indicated, the number of motile trypanosomes in each well was assessed with the use of a counter chamber. The mTNF was preincubated or not for 1 hour with either *T. brucei brucei* soluble extract (10 μg/ml), *N,N'*-diacetylchitobiose (1 μg/ml), or rabbit antibody to mTNF-tip (anti–mTNF-tip; 10 μg/ml). A similar preincubation was done with irrelevant control rabbit antiserum (10 μg/ml), but this treatment had no effect on the trypanocidal or tumoricidal activities of m/hTNF shown in Fig. 1. We generated anti–mTNF-tip by injecting rabbits on day 0 with 50 μg of a complex consisting of 43 μg of avidin (NeutraLite) with 7 μg of NH_2-terminal biotinylated mTNF-tip peptide in Freund's complete adjuvant (FCA). On day 22 the rabbits were injected with 50 μg of the complex in Freund's incomplete adjuvant (FIA) followed on day 44 by a booster injection of 100 μg of the complex in PBS at similar molar ratios. The antisera were collected 10 days after the booster injection and purified on a protein G–Sepharose column.
22. Single-letter abbreviations for the amino acid residues are as follows: A, Ala; C, Cys; D, Asp; E, Glu; G, Gly; K, Lys; L, Leu; P, Pro; Q, Gln; R, Arg; T, Thr; W, Trp; and Y, Tyr.
23. The specific activity on L929 cells, as titrated according to the standard procedure [L. Fransen, J. Van der Heyden, R. Ruysschaert, W. Fiers, *Eur. J. Cancer Clin. Oncol.* **22**, 419 (1986)], was 1.8×10^8 U/mg for mTNF, 2×10^7 U/mg for hTNF, and 10^7 U/mg for hLT. The mTNF was preincubated or not for 1 hour as described (*21*).
24. The in vitro trypanolysis assay was done as described in Fig. 1A. The TNF-derived peptides were synthesized with the use of Fmoc.– α-amino group protection and T-butyl side chain protection [G. B. Fields and R. L. Noble, *Int. J. Pept. Protein Res.* **35**, 161 (1990)]. Subsequently, the peptides were purified with a C_{18} reversed-phase high-performance liquid chromatography column. The peptides synthesized were as follows: mTNF-tip peptide (mtip), CGPKDTPEGAELKPWYC; hTNF-tip peptide (htip), CGQRETPEGAEAKPWYC; tip subpeptide, CTPEGAEC (*22*). Alanine substitution mutants of the tip subpeptide were as follows: mutant 1 (m1), CAPEGAEC; mutant 2 (m2), CTAEGAEC; mutant 3 (m3), CTPAGAEC; mutant 4 (m4), CTPEAAEC; mutant 5 (m5), CTPEGAAC. To retain theoretically the original free mTNF conformation as much as possible, we replaced Ser^{99} of the mTNF-tip peptide by Cys, and Cys^{100} by Gly so that a disulfide bridge could

be formed between Cys^{99} and Cys^{115} in the mTNF-tip peptide. Similarly, a disulfide bridge between Cys^{100} and Cys^{116} was introduced in the tip peptide of hTNF. We synthesized the tip subpeptides with NH_2- and COOH-terminal cysteines in order to investigate the effect of ring closure on peptide activity. In contrast to the mTNF and hTNF tip peptides, these short peptides were very difficult to close by air oxidation, and no closure could be demonstrated within the time span of these experiments. The oxidized (closed) forms of these subpeptides were inactive (*10*). Furthermore, the peptide TPEGAE was synthesized and found to have an activity indistinguishable from that of tip subpeptide in its reduced (open) form (*10*).

25. For expression of mature mTNF in *Escherichia coli*, mature mTNF cDNA was fused exactly to an ATG codon in the expression vector pIG2 (Innogenetics, Ghent, Belgium). The T104A, P105A, and del(T^{104}–E^{109}) mutations were introduced directly into this vector by a variation on the cassette-mutagenesis method [J. A. Wells *et al.*, *Gene* **34**, 315 (1985)] with the use of synthetic oligonucleotides. The oligonucleotides used for the construction of mTNF(T104A) were 5′-CAAGGACGCTCCGGAGGGGGCTGAGCT-3′ and 5′-CAGCCCCCTCCGGAGCGTC-3′; for the construction of mTNF(P105A), 5′-CAAGGACACCGCTGAGGGCGCCGAGCT-3′ and 5′-CGGCGCCCTCAGCGGTGTC-3′; and for the construction of mTNF[del(T^{104}–E^{109})], 5′-CAAGGACCTCAAACCATGGTATGAGCCCATATAC-3′ and 5′-ATGGGCTCATACCATGGTTTGAGGTC-3′. Expression was carried out in *E. coli* strain MC1061(pcl857) [K. F. Wertman *et al.*, *Gene* **49**, 253 (1986); E. Remaut *et al.*, *ibid.* **22**, 103 (1983)].

26. We thank F. Bosman and M. Verhaeghe for the purification of the TNF mutants and S. Pattijn for the TNF bioassays; A. Van Broekhoven for the fermentation of the *E. coli*–produced mutants and H. Smets for peptide synthesis; D. Wallach for providing shTNF-RI, J. Bouckaert and R. Loris for *Urtica dioica* lectin, Ph. Stas and J. Pletinckx for help with molecular graphics, E. Vercauteren for administrative support, and A. Van de Voorde and F. Shapiro for useful discussions. Supported by the UNDP/World Bank/World Health Organization Special Program for Research and Training in Tropical Diseases, the Fonds voor Geneeskundig Wetenschappelijk Onderzoek (30072.88), and the Vlaams Aktieprogramma Biotechnologie research program.

29 September 1993; accepted 7 December 1993

Mesodermal Patterning by a Gradient of the Vertebrate Homeobox Gene *goosecoid*

Christof Niehrs, Herbert Steinbeisser, Eddy M. De Robertis*

Amphibian mesoderm arises from the marginal zone of the early gastrula and generates various tissues such as notochord, muscle, kidney, and blood. Small changes (twofold) in the amount of microinjected messenger RNA encoding the *goosecoid* (*gsc*) homeodomain protein resulted in marked changes in the differentiation of mesoderm in *Xenopus laevis*. At least three thresholds were observed, which were sufficient to specify four mesodermal cell states. Endogenous *gsc* messenger RNA was expressed in the marginal zone in a graded fashion that is congruent with a role for this gene in dorso-ventral patterning of mesoderm at the early gastrula stage.

Concentration gradients of molecules that elicit multiple discontinuous cellular responses at different threshold concentrations have been shown to play important roles during *Drosophila* embryogenesis (*1*). The view that concentration gradients of molecules might pattern mesodermal tissues in vertebrates has recently gained support from the discovery that uncommitted embryonal animal cap cells from *Xenopus* can respond to the peptide growth factor activin, giving rise to various mesodermal cell types at distinct threshold concentrations (*2*, *3*). However, it is not known whether activin molecules are present in a graded manner at the right time and place during mesoderm specification. The homeobox gene *goosecoid* (*gsc*) was cloned from a dorsal lip complementary DNA (cDNA) library and was shown to encode a DNA-binding protein with a DNA-binding specificity similar (*4*), but not identical (*5*), to that of the *Drosophila* anterior morphogen *bicoid*. The *gsc* gene is expressed in the Spemann organizer of *Xenopus* embryos and is a primary response gene inducible by activin in the absence of protein synthesis (*6*). Its misexpression in ventral mesoderm is sufficient to induce morphogenetic movements and secondary embryonic axes (*6*, *7*). Here we show that *gsc*, which is expressed at the right time and place for mesoderm specification, can pattern mesodermal differentiation through a concentration gradient.

Xenopus laevis embryos were injected with serial twofold dilutions of synthetic *gsc* mRNA; for each experiment, all eight vegetal blastomeres of a 16-cell stage embryo were injected. Embryos were cultured until the early gastrula stage, at which time ventral marginal zone (VMZ) explants were prepared. Explants were then cultured for 2.5 days until sibling embryos reached the tadpole stage (*8*). Increasing doses of *gsc* mRNA led to the inhibition of blood differentiation [the normal self-differentiation of VMZs (*9*)] and to the appearance of successive peaks of pronephros, muscle, notochord, and neural tissue (Fig. 1). These results showed that *gsc* is able to dorsalize the VMZ in a highly dose-dependent manner and suggested that discontinuous responses might underlie these tissue transitions.

To reveal the existence of concentration thresholds in the action of *gsc* mRNA, we analyzed the expression level of various marker genes in injected VMZ explants by quantitative polymerase chain reaction (PCR) (*10*). Explants cultured until sibblings were neurulae (Fig. 2A) show the following: (i) The expression of α-globin, typical of ventral cells (*11*), is turned off by *gsc*. (ii) The *Xenopus* homolog of the *brachyury* gene (*Xbra*), expressed normally in both ventral and dorsal cells (*12*), is induced over basal levels by small amounts of *gsc*. (iii) A *Xenopus* homolog of the *Hox* gene *labial*, *Xlab* (*4*), is induced by *gsc*. (iv) Cardiac actin, expressed in myotomes (*13*), is induced by moderate amounts of *gsc* mRNA. Sufficient *Xbra* mRNA can lead to muscle differentiation in animal caps (*14*), which raises the possibility that *gsc* might induce muscle by acting on *Xbra*. (v) UVS.2, a metalloprotease expressed dorsoanteriorly in hatching gland tissue (*15*), is induced with intermediate amounts and repressed with larger amounts of *gsc* mRNA, as is actin. (vi) Endogenous *gsc*, which at the neurula stage is expressed in head mesoderm (*16*) [the most dorso-anterior mesoderm (*3*)], is induced exclusively at the highest doses of *gsc* mRNA. Endogenous *gsc*, and not microinjected *gsc* mRNA, is detected in these PCR assays because the 5′ PCR primer we used hybridizes to a sequence in the 5′ untranslated region that is deleted in the injected *gsc* RNA (*10*). Autoactivation, such as that observed here, is a property expected of genes that generate stable cell states (*1*). (vii) Histone H4 (*17*) remains unaffected by *gsc* injection and was used as a reference. All PCR assays were carried out at cycle numbers below amplification-saturation levels, which were determined empirically for each primer pair (*10*).

We conclude that as little as a twofold difference in *gsc* concentration can affect cell fate after microinjection of *gsc* mRNA. Thus, sharp thresholds appear for *Xbra*, cardiac actin, and endogenous *gsc* at 2.5, 5, and 10 pg per blastomere, respectively (Fig. 2A). This defines at least four states of cell differentiation within an eightfold concentration range (1.25 to 10 pg per blastomere). The results do not, however, distinguish whether the genes analyzed are directly affected by the *gsc* DNA-binding

Molecular Biology Institute and Department of Biological Chemistry, University of California, Los Angeles, CA 90024–1737, USA.

*To whom correspondence should be addressed.